JOURNAL OF NANO- AND ELECTRONIC PHYSICS
Vol. **5** No 2, 02029(4pp) (2013)

ЖУРНАЛ НАНО- ТА ЕЛЕКТРОННОЇ ФІЗИКИ
Том **5** № 2, 02029(4cc) (2013)

Preparation and Characterization of Antimony Doped Tin Oxide Thin Films Synthesized by Co-Evaporation of Sn and Sb using Plasma Assisted Thermal Evaporation

C. Jariwala[1,*] M. Dhivya[1,2], R. Rane[1], N. Chauhan[1], P.A. Rayjada[1], P.M. Raole[1], P.I. John[1]

[1] *Institute for Plasma Research, A-10/B, GIDC Electronics Estate, Sector-25, Gandhinagar 382016 Gujarat, India*
[2] *Kanchi Mamunivar Center for Post Graduate Studies, Pondicherry University, Puducherry-605008 Puducherry, India*

(Received 15 February 2013; revised manuscript received 03 May 2013; published online 04 May 2013)

Tin oxide (SnO_2) thin films are having promising properties such as high visible transmittance and low electric resistivity, makes them very important transparent conductor in a variety of optoelectronics devices. Further, doping with pentavalent impurity such as Antimony (Sb) enhances its conductivity considerably. In order to study the effect of Antimony doping, Antimony doped tin oxide (SnO_2 : Sb) thin films have been prepared by the co-evaporation of Sn and Sb using Plasma Assisted Thermal Evaporation (PATE) in oxygen (O_2) partial pressure at various doping level from 4% to 25%. The influence of various Sb doping levels on the compositional, electrical, optical and structural properties have been investigated using Energy Dispersive X-ray (EDX) spectroscopy, Ultraviolet-Visible (UV-VIS) transmission spectroscopy, four-probe resistivity measurement and X-ray Diffraction (XRD), respectively. EDX studies confirmed the different Sb doping levels in the grown films from 4 % to 25 %, while electrical resistivity is obtained in range of 0.36 to 9.5 Ohm·cm using four-probe setup for 4 % to 25 % Sb doping levels. Transmittance spectra measured in UV-VIS range for Sb doped films show reduction in an average transmittance in respect to increase in Sb doping levels in the grown films. Whereas, XRD analysis reveals that higher Sb doping of 25 % induce the precipitation of antimony oxide (Sb_2O_3) phase and its precipitation suppressed the growth of SnO_2 peaks as well as responsible for reduction in conductivity and transparency. The best electrical resistivity of optimized SnO_2 : Sb (5 %) is 0.36 Ohm·cm without deteriorating the high (~ 80 %) average transmittance in the wavelength region 300-800 nm in comparison to undoped SnO_2 film (6.57 Ohm·cm) , confirm the usefulness of SnO2 : Sb (5 %) films for device applications.

Keywords: Transparent Conducting Oxide, Antimony Doped Tin Oxide Thin Films, Co-Evaporations, Plasma Assisted Thermal Evaporation, Optical Properties, X-Ray Diffraction, Electrical Properties, Scanning Electron Microscopy.

PACS numbers: 81.05.Gh, 81.15.Gc, 52.77 Dq

1. INTRODUCTION

Transparent Conducting Oxides (TCOs) like In_2O_3, SnO_2, ZnO, In_2O_3 : Sn etc are employed as transparent electrode in solar cells, flat-panel displays, light emitting diodes, electro chromic windows, gas and chemical sensors due to their promising properties[1]. Among these TCO's, In_2O_3 : Sn also referred as Indium Tin Oxide (ITO) is most widely used TCO due to its high visible transmittance (~ 90 % at 550 nm), low electrical resistivity ($\sim 2 \times 10^{-4}$ Ω·cm), and relatively high work function (≈ 4.8 eV) [1]. However, ITO is an expensive TCO since indium in ITO is a rare and expensive element. Therefore, a lot of effort has been directed to develop more economical alternative TCO materials such SnO_2 : Sb. Impurity doped SnO_2 is cheaper and easier to fabricate than ITO. Thus, impurity doped SnO_2 is more favorable than ITO in various fields such as solar cells, optoelectronics devices, flat panel displays and gas sensors [1].

SnO_2 : Sb thin films have been prepared by various methods like activated reactive evaporation [2], Plasma enhanced-CVD [3], Electroless deposition [4], Radio frequency (RF) [5], and Direct Current (DC) magnetron sputtering [6], Electron beam evaporation (e-beam) [7], Sol Gel technique [8, 9], Spray Pyrolysis [10], and hydrothermal method [11]. In present study, SnO_2 : Sb thin films are deposited by co-evaporation of Sb and Sn using PATE technique. The effects of dopant concentration on electrical, optical and structural properties are studied over a considerable range from 0 to 25 % of Sb content in the grown films. The detail optical, structural, compositional and electrical analysis of the deposited films have been performed using optical transmission spectroscopy, XRD, EDX, SEM and Four-probe setup respectively.

2. EXPERIMENTAL

SnO_2 : Sb films are deposited on pre heated (350-375 °C) glass and double side polished silicon wafers by coevaporating metallic tin (Sn, 99.80 %, supplied by Acros Organics, USA) and antimony(Sb, 99 + %, supplied by Acros Organics, USA) in the presence of O_2 plasma. The vacuum chamber is evacuated to base pressure of 2×10^{-5} mbar prior to each deposition. O_2 plasma is formed using RF (13.56 MHz) supply connected between the resistively heated molybdenum boats and substrate (separated by 10 cm) in order to enhance the reaction of evaporating Sn, Sb atoms with O_2. The O_2 partial pressure is kept fixed to 10^{-3} mbar and Sb doping level in the deposited films is varied by varying the current applied to the corresponding molybdenum boat. The schematic of experimental set up is shown in Fig. 1 and further experimental details are mentioned in our recent published work [12].

* chetan@ipr.res.in

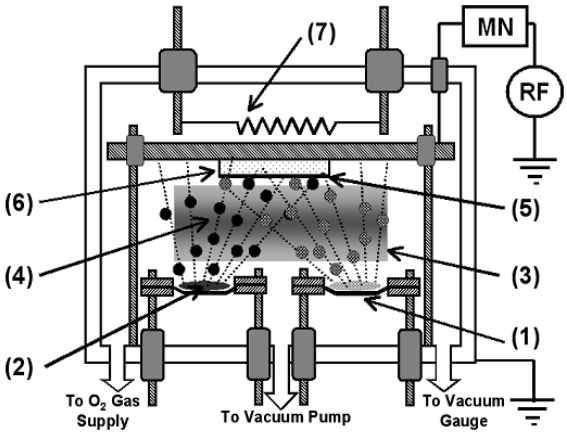

Fig. 1 – A schematic diagram of dual source Plasma Assisted Thermal Evaporation for antimony doped tin oxide thin film depositions: 1) Evaporation boat; 2) Source material; 3) Oxygen plasma; 4) Evaporated atoms; 5) Deposited thin film; 6) Substrate; 7) Substrate heater. MN = Matching network; RF = 13.56 MHz supply

The optical transmission of the deposited films are measured in the wavelength region of 280-800 nm of the spectrum using Spectrophotometer (Shimadzu UV-VIS 1800). The crystallinity of the films are investigated using Cu-K_α radiation (Rich Seifert make model XRD 3000PTS). The electrical properties are measured by four point probe at room temperature with linear contact geometry using spring-loaded probes pressing on the film surface. SEM (440i, LEO make, UK) used to study surface morphology and thickness of films by cross-sectional measurement, whereas elemental analysis performed with EDX analysis (7060, Oxford make, UK).

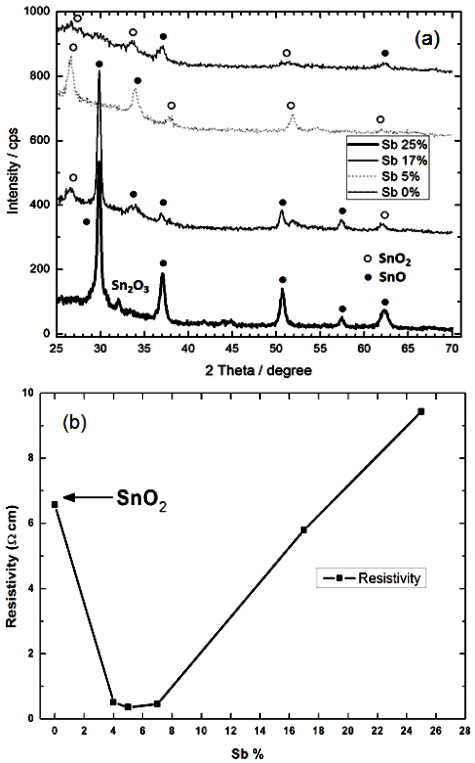

Fig. 2 – SnO_2 : Sb films deposited on glass substrates by co-evaporation of Sb and Sn using PATE (a) XRD patterns and (b) Resistivity dependence for different Sb doping levels ranging from 0 to 25 %

3. RESULTS AND DISCUSSION

XRD patterns obtained for SnO_2 : Sb films at different doping levels of Sb grown at 375 ºC are shown in Fig. 2a. For undoped (i.e. SnO_2) films grown by PATE, the preferred orientation is SnO_2 (110) with rutile structure and it contains both SnO and SnO_2 phases. With low levels doping of Sb (4 to 7 %), there is no significant change in the XRD pattern, which could be due to the substitution of Sn atoms by Sb in the SnO_2 lattice (only for Sb 5 % XRD shown in the Fig. 2a). As the doping level of Sb is increased to 17 %, a peak attributed to SnO (101) phase at 29.86 enhanced drastically. Also, with this doping level SnO_2 peaks are suppressed which is evident from the XRD spectra. Further increment in the Sb doping level of 25 %, a new peak at 32.02 arises and it is identified as Sb_2O_3, belongs to antimony oxide, as also suggested in the literature owning to higher dopant level of Sb. Due to this high doping of Sb, the growth of SnO_2 phase is further suppressed in the grown films. This suppression might be due to the precipitation of the antimony oxide as reported in the literature [13, 14, 15].

The effect of Sb doping on resistivity of deposited films are measured by four probe shown in the Fig. 2b. It is observed from the plot that at low doping levels of Sb up to 5 % the resistivity decreases and at high doping level from 7 to 25 %, the resistivity increases. On other hand the resistivity of undoped (i.e. SnO_2) film is 6.57 Ω·cm, which is very large. It is noted from the plot that doping with Sb of 5 %, the value of resistivity falls sharply to 0.36 Ω·cm from undoped value (i.e. 6.57 Ω-cm). Further, increase in Sb content from 7 to 25 %, resistivity sharply increase from 0.43 to 9.43 Ω·cm. Hence, in the initial stages, Sb doping increases the carrier concentration and mobility, which is resulted in lowering of the resistivity. The increase in carrier concentration could be due to the substitutional doping of SnO atoms in SnO_2 lattice by replacing Sn atoms and contribute more electrons for conduction (acting as donor). It is also reported that the initial decrease in resistivity is due to the substitution of Sn^{4+} by Sb^{5+} in the SnO_2 lattice as their ionic radii are matching at low doping levels of Sb, which act as a donor and hence there will be increase in the carrier concentration. [6, 10, 16, 17].

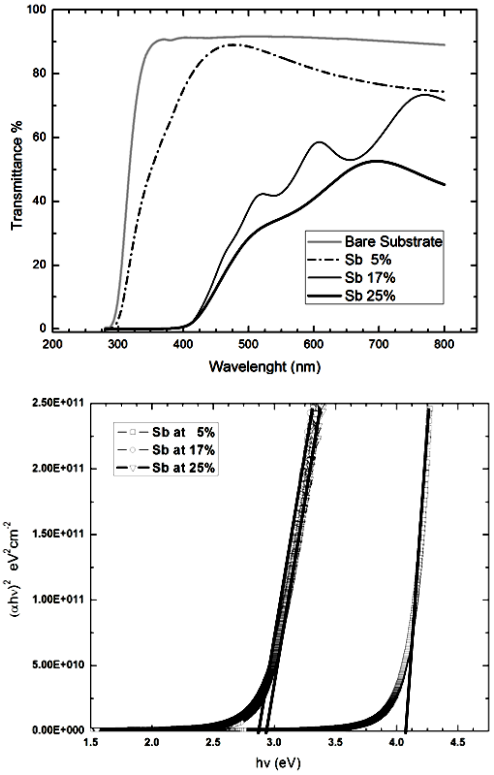

Fig. 3 – (a) Optical transmission spectra and (b) the plot of $(\alpha hv)^2$ against hv for $SnO_2:Sb$ films deposited on glass substrates with various doping levels of Sb

Fig. 3a shows optical transmittance spectra of $SnO_2:Sb$ films for different Sb levels (5, 15, and 25 %) measured in the wavelength range from 280-800 nm. It is observed from the Fig. 3a that transmittance is high (≈ 80 %) for the thin films deposited at low doping levels of Sb (5 %). Whereas, further increase in the Sb doping level to 15 %, transmittance drastically reduces to ≈ 50 % and resulted in a large variation in the absorption edge, shifted towards longer wavelength region. Further increase in the Sb doping to 25 %, the transmittance reduces further to ≈ 30 %. In order to determine the optical band gap of the deposited $SnO_2:Sb$ films, a graph is plotted between $(\alpha hv)^2$ and hv shown in Fig. 3b. An extrapolation of the straight-line portion of the plot to the energy (hv) axis gives optical band gap values of the deposited $SnO_2:Sb$ films. From the Fig. 3b, it is observed that optical band gap of the deposited films reduce with the increase in the Sb doping level from ≈ 4.1 eV for 5 % Sb to ≈ 2.9 and 2.8 eV for 17 and 25 % Sb, respectively.

A typical EDX spectrum obtained for $SnO_2:Sb$ films are shown in Fig. 4a, confirm the presence of Sb element in all co-evaporated films. The atomic weight percentages of Sb in these films are calculated through area under the curve analysis of peaks belongs of Sn and Sb. A cross-section SEM image (Fig. 4b) shows the total thickness of films prepared by co-evaporation Sb and Sn by PATE. In present study, all films are grown at 2-3 nm/sec deposition rates.

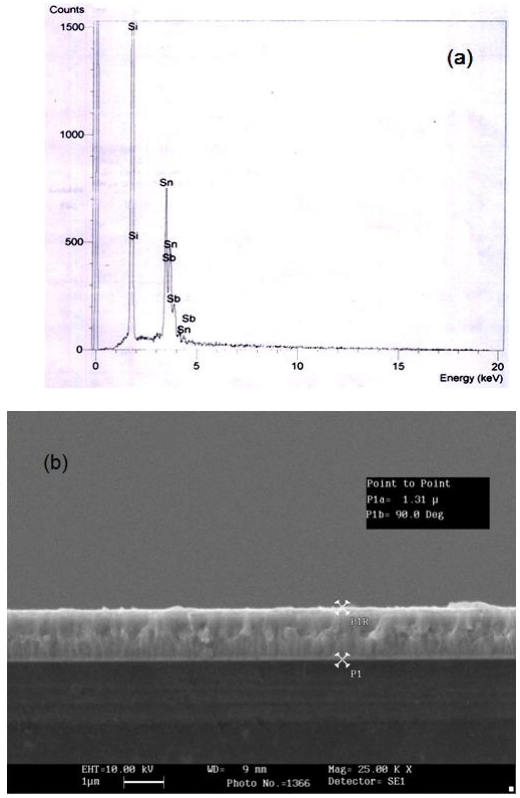

Fig. 4 – (a) a typical EDX spectrum obtained from $SnO_2:Sb$ thin films on silicon wafers by EDX analysis and (b) SEM cross section view of $Sb:SnO_2$ thin film deposited by co evaporation of Sb and Sn

4. CONCLUSION

We have investigated optical, structural and electrical properties of $SnO_2:Sb$ films with different Sb doping levels deposited by co-evaporation of Sn and Sb using PATE at substrate temperature in the range of 350-375 °C. With low level Sb doping, the electrical resistivity is enhanced greatly, while maintaining high optical transmittance ≈ 80 % in the range of 300-800 nm. The best resistivity 0.36 Ω·cm has been obtained for 5 % Sb doping level without deteriorating optical transmittance of the grown $SnO_2:Sb$ thin films. Further, increase in Sb doping levels enhanced resistivity and reduce optical transmittance for doping levels 7 to 25 % in the $SnO_2:Sb$ films. While, XRD analysis has revealed the Sb_2O_3 phase present in the films at high Sb doping (25 %), which could be the source for enhancement of resistivity. The investigations about $SnO_2:Sb$ films have identified the critical role of Sb dopant for achievement best quality TCO, which can be replacement for ITO films for various optoelectronics device applications.

ACKNOWLEDGEMENT

We thank Dr. A. Chainani for valuable suggestions for SnO_2 thin film deposition activity at IPR, Gandhinagar, India.

REFERENCES

1. H.L. Hartnagel, A.L. Dawar, A.K. Jani, C. Jagadish, *Semiconduction Transparent Thin Films* (Bristol and Philadelphia: Institute of Physics Publishing: 1995).
2. H.S. Randhawa, M.D. Matthews, R.F. Bunshah, *Thin Solid Films* **83**, 267 (1981).
3. P.Y. Liu, J.F. Chen, W.D. Sun, *Vacuum* **76**, 7 (2004).
4. D. Raviendra, J.K. Sharma, *J. Phys. Chem. Solids* **46**, 945 (1985).
5. Hong-Lei Ma, Xiao-Tao Hao, Jin Ma, Ying-Ge Yang, Jie Huang, De-Heng Zhang, Xian-Gang Xu, *Appl. Surf. Sci.* **191**, 313 (2002).
6. J. Montero, J. Herrero, C. Guillen, *Sol. Energ. Mat. Sol. C.* **94**, 612 (2010).
7. H.A. Mohamed, *Optoelectron. Adv. Mat.* **3**, 936 (2009).
8. Viviany Geraldo, Luis Vicente de Andrade Scalvi, Evandro Augusto de Morais, Celso Valentim Santilli, Sandra Helena Pulcinelli, *Mater. Res.* **6**, 451 (2003).
9. Jing Kong, Hongmei Deng, Pingxiong Yang, Junhao Chu, *Mater. Chem. Phys.* **114**, 854 (2009).
10. Shanthi, C. Subramanian, P. Ramasamy, *J. Cryst. Growth* **197**, 858 (1999)
11. Thanh Binh Nguyen, Thi Thanh Binh Le, Ngoc Long Nguyen, *Adv. Nat. Sci.: Nanosci. Nanotechnol.* **1**, 025002 (2010).
12. C. Jariwala, T. Garg, R. Rane, N. Chauhan, P.A. Rayjada, C.J. Panchal, P.I. John, *J. Nano- Electron. Phys.* **3** No 1, 318 (2011).
13. Keun-Soo Kim, Seog-Young Yoon, Won-Jae Lee, Kwang Ho Kim, *Surf. Coat. Tech.* **138**, 229 (2001).
14. B. Grzeta, E. Tkalcec, C. Goebbert, M. Takeda, M. Takahashi, K. Nomura, M. Jaksic, *J. Phys. Chem. Solids* **63**, 765 (2002).
15. Talaat M. Hammad, Naser K. Hejazy, *Int. Nano Lett.* **1**, 123 (2011).
16. M. Kojima, H. Kato, M. Gatto, *J. Non-Cryst. Solids* **218**, 230 (1997)
17. C. Terrier, J.P. Chatelon, J.A. Roger, *Thin Solid Films* **295**, 95 (1997).